Heavy-quark production with k_t factorization: The importance of the sea-quark distribution

Benjamin Guiot*

Departamento de Física, Universidad Técnica Federico Santa María; Casilla 110-V, Valparaiso, Chile

(Received 14 December 2018; published 8 April 2019)

We discuss the fact that k_t-factorization calculations for heavy-quark production include only the $gg \to Q\bar{Q}$ contribution. The cases of fixed-flavor-number scheme and variable-flavor-number scheme calculations are analyzed separately. For the latter, we show that, similarly to the collinear factorization, the main contribution is given by the $Qg \to Qg$ process. In this scheme, calculations including only the gg contribution should show a large discrepancy with the data. We show that, if they do not, it is because they include (effectively) a large K factor.

DOI: 10.1103/PhysRevD.99.074006

I. INTRODUCTION

Heavy flavor is an important tool for the study of strong interaction and QCD matter. One reason being that it makes theoretical calculations simpler, in particular because the heavy-quark mass allows for the use of perturbation theory. The energy loss of a heavy quark propagating in a medium has been studied extensively, and it is used to determine some of the medium properties, like the transport coefficient $\hat{q}$. If using a transport code, the heavy quark mass allows to use equations which are simplified versions of the Boltzmann equation. It is a privileged probe for the study of the quark-gluon plasma, since, contrary to light particles, it is generally accepted that it cannot be produced significantly in the hot medium. Then, the only source of heavy quarks is the hard process, calculable in perturbation theory. From the experimental side, heavy flavors give a clear signal, and experiments like ALICE are able to see the secondary vertex for D mesons.

Having a good understanding of heavy-quark production is then of first importance for the phenomenology. In this paper, we concentrate on the p_t distribution of a heavy quark. More exclusive processes, like quarkonia production, are not considered. We treat the case of collinear factorization in Sec. II, where the differences between a fixed-flavor-number scheme and a variable-flavor-number scheme are discussed. Some common statements on heavy-quark production will be analyzed, and it is reminded [1] that, in a variable-flavor-number scheme,[1] some of them are wrong. In particular, it is generally not true that the gluon fusion process gives the main contribution. In the region $p_t > m$, m being the heavy-quark mass, it is in fact given by the $Qg \to Qg$ process.

In Sec. III, we present the usual k_t-factorization formula for heavy-quark production. The main goal of this paper is to discuss the fact that k_t-factorization calculations take into account only the $gg \to Q\bar{Q}$ process. After some remarks, in Sec. IV, we analyze separately the cases of fixed-flavor-number scheme and variable-flavor-number scheme calculations, Secs. V and VI. We will see that the situation is similar to the collinear factorization case. When the variable-flavor-number scheme is used, the main contribution is given by the $Qg \to Qg$ process. The gg contribution alone *should not* gives a satisfying description of the data. If it does, it means that the calculation (effectively) includes a incorrect large K factor, and we will see how it can be "implemented." At the end of Sec. VI, numerical calculations using a variable-flavor-number scheme, including flavor excitation processes, are presented.

II. HEAVY FLAVOR PRODUCTION WITHIN THE COLLINEAR FACTORIZATION

For hadron-hadron collisions, the collinear factorization formula reads [2]

$$\frac{d\sigma}{dx_1 dx_2 d^2p_t}(P_1,P_2) = \sum_{i,j} f^i(x_1,\mu_f^2) f^j(x_2,\mu_f^2) \hat{\sigma}^{ij}\left(x_1x_2s, p_t, \alpha_s(\mu_R), \frac{Q^2}{\mu_R}, \frac{Q^2}{\mu_f}\right), \tag{1}$$

*benjamin.guiot@usm.cl

[1]This scheme is probably the most commonly used at LHC energies.

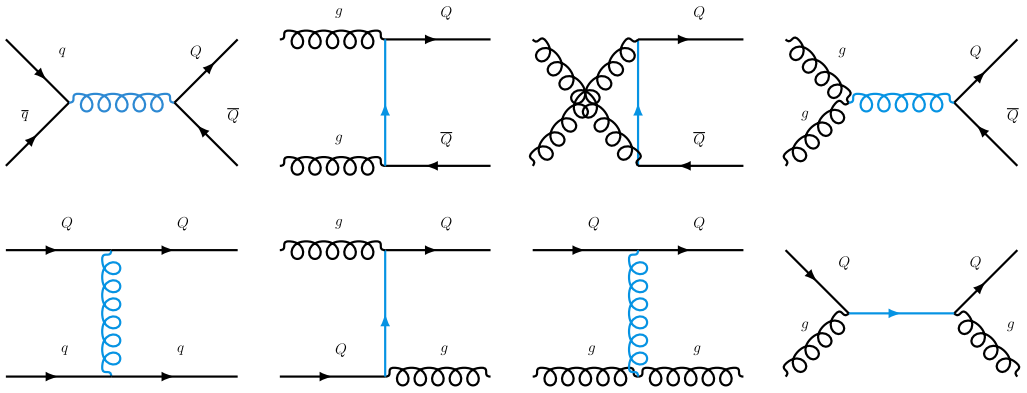

FIG. 1. Leading order Feynman diagrams with an outgoing heavy quark Q in the VFNS. We neglect contributions implying two incoming heavy quarks like $c\bar{c} \to c\bar{c}$ or $cb \to cb$.

with $s = (P_1 + P_2)^2$, P_k the hadron 4-momentum and x_k the longitudinal momentum fraction of the hadron carried by the incoming parton:

$$x_1 = \frac{p_t}{\sqrt{s}} e^{y_a} + \frac{p_t}{\sqrt{s}} e^{y_b} \qquad x_2 = \frac{p_t}{\sqrt{s}} e^{-y_a} + \frac{p_t}{\sqrt{s}} e^{-y_b}, \tag{2}$$

with y_a and y_b the rapidities of the two outgoing partons and p_t their transverse momentum.[2] The hard scale is denoted by Q^2 and is conventionally chosen[3] to be p_t^2. The factorization and renormalization scales are μ_f and μ_R, respectively. They are sometimes chosen to be equal, but it is not necessary, and in FONLL calculations [4], they are varied independently in order to estimate the corresponding uncertainties. The partonic cross sections, $\hat{\sigma}^{ij}$, depend also on the mass of the heavy partons involved in the hard process, and have a perturbative expansion:

$$\hat{\sigma} = \sum_{k=0}^{\infty} \alpha_s^{n+k} \hat{\sigma}^k, \tag{3}$$

with n the power of α_s at leading order. In the case of heavy-quark production, $n = 2$. The functions f^i are the parton densities.

A. Fixed-flavor-number scheme

In Eq. (1), in order to know if the sum over the indices i and j includes the heavy quarks, one has to specify the scheme and the scale μ_f. Historically, the first next-to-leading order (NLO) calculations have been done using the fixed-flavor-number scheme (FFNS) [5–8]. The 3-flavor scheme assumes that the nucleon is made only of gluons and three light quarks, while the 4-flavor scheme, which can be used for bottom production, also includes the charm quark. Then, LO calculation includes only the flavor creation diagrams shown in the upper row of Fig. 1. It is known [4,9,10] that this scheme fails at $p_t \gg m_Q$, because of the absence of resummation of the large logarithm $\ln(p_t^2/m_Q^2)$. This issue is solved by the variable-flavor-number scheme (VFNS), presented in the next section. However, within uncertainties (which are large in this scheme), the NLO FFNS calculations are in good agreement with data up to quite large p_t. For instance, in Ref. [11], Figure 2 (left panel), we observe the agreement of the NLO calculation for bottom production on the full p_t range ([0,25] GeV).

The situation is completely different in the case of FFNS LO calculations. Using the same gluon density, a large K factor is necessary to bring agreement with NLO calculations, as discussed in [6]. In this paper, it is shown (Fig. 12) that at $\sqrt{s} = 1.8$ TeV, for the bottom mass,

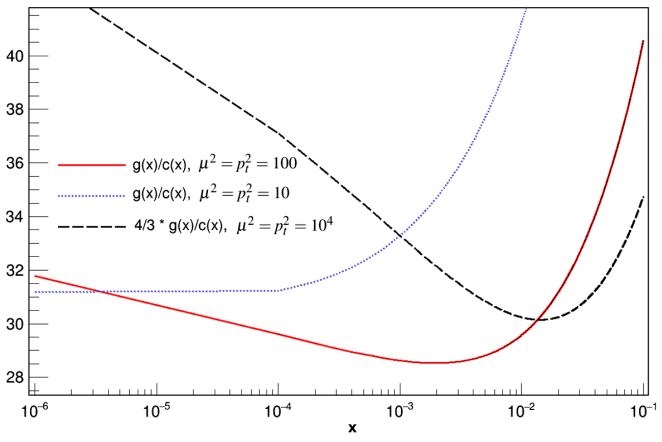

FIG. 2. Ratio $g(x,\mu^2)/c(x,\mu^2)$ for different μ^2 values, in GeV^2. We use the CTEQ14 PDF at NLO [12]. It is reminded that for $d\sigma/dp_t$, one usual choice is $\mu_f^2 = p_t^2$.

[2]In this study, we will not consider higher order corrections to the partonic cross sections, $\hat{\sigma}^{ij}$. Then, the two outgoing partons are back to back, both in the partonic center-of-momentum frame and in the laboratory frame. This will not be true anymore when using the k_t factorization, since the transverse momentum, k_t, of the incoming partons is taken into account. In fact, it is one of the interests of this formalism.

[3]See Ref. [3] for a detailed discussion on this choice.

$K = 2.5$. The reason for this large factor is not really the "large" logarithm, but the fact that NLO contributions open the flavor excitation channels, which have large cross sections.

Preparing the discussion on unintegrated parton densities, we note that in [6], the LO calculations without the K factor are below the data.[4] But the parton distribution functions (PDFs) are order- and scheme-dependent quantities, and with the choice $g(x,\mu^2)^{LO} = \sqrt{2.5}g(x,\mu^2)^{\mathrm{NLO}}$, the LO FFNS calculation for bottom production at the Tevatron works perfectly fine, since the LO and NLO lines have a similar slope, see [6], Figure 12. However, in [6], Figure 10, we can see that at the same energy, but with a heavy-quark mass $m_Q = 80$ GeV, the K factor is only 1.5, so our new LO FFNS gluon will do a poor description of the (hypothetical) data. It will result in large uncertainties on the LO FFNS gluon distribution, which is expected since the $\ln(p_t^2/m_Q^2)$ and the flavor excitation cross sections, which partially explain the difference between $m_Q = 5$ and $m_Q = 80$ GeV, are not at all included.

In order to describe heavy-quark production data, using gluon densities with reasonable uncertainties, one should (at least) work either with the FFNS at NLO or with the VFNS at LO.

B. Variable-flavor-number scheme

Even at NLO, calculations using the FFNS do not work quite well at $p_t \gg m_Q$. In this region, it is necessary to resum the large logarithms $\ln(p_t^2/m_Q^2)$. This is achieved with the VFNS, which includes the heavy-quark density and takes into account the flavor excitation diagrams, even at LO. This scheme is used by the GM-VNFS [10,13] and FONLL [4] calculations, which include also the resummation of large logarithms due to final state emissions, using scale-dependent fragmentation functions.

The VFNS has several advantages. For $p_t > m_Q$, LO calculations give results comparable to the FFNS NLO calculations, as shown in the next subsection. Compared to the FFNS, the uncertainties due to scale variation are smaller [11]. Finally, the uncertainties on the gluon densities are also smaller, and going from LO to NLO does not change significantly their value (for $\mu >$ few GeV, see the two black curves in Fig. 5), contrary to the FFNS case.

C. Analyzing some common statements on heavy-quark production

In the VFNS, one has to take into account the heavy-quark densities, and we can wonder which process gives the main contribution. For the second part of this paper, about the p_t distribution of a heavy quark within k_t factorization, it is useful to analyze first the following common statements in the framework of collinear factorization:

(1) At small x, the main contribution comes from $gg \to Q\bar{Q}$.
(2) At small x, the gluon distribution is much larger than the charm distribution.
(3) The gluon distribution grows faster than the quark distribution towards small x (see for instance [14]).
(4) At leading order, one needs a K factor to take into account higher orders corrections ($K > 2$).

It is important to understand that there are some implicit statements. For instance, statement 3 is sometimes considered to explain statement 2, and statement 2 is considered to explain statement 1.

We will not discuss the correctness of statement 3, since it is a general result of evolution equations [14] [Eq. (2.124) and discussion thereafter]. On the contrary, it is wrong to think that statement 3 implies statement 2, and it is easy to find a counterexample. Consider the two linear functions $f_1(y) = y$, with slope one, and $f_2(y) = 2 + 2y$ with slope two. Even if f_2 grows faster than f_1, the ratio f_2/f_1 decreases with y. In Fig. 2, we show the ratio $g(x,\mu^2)/c(x,\mu^2)$ for different μ^2 values, obtained with the CTEQ14 PDFs at NLO [12] (table CT14n.00.pds). We see that for $\mu^2 = 10$ GeV^2, the ratio decreases towards small x. For $\mu^2 = 100$ GeV^2 the situation is more complicated since it depends on the x range. We first have a fast decrease between $x = 0.1$ and $x = 0.001$. Then, the ratio starts to increase but very slowly. For $\mu^2 = 10^4$ GeV^2, the increase is faster but this curve corresponds to energies much higher than LHC energies. Generally, one can conclude that even if statement 3 is true, it is incorrect to use it in order to justify statement 2. This ratio is large since the beginning, that is all.

We have seen that statements 3 and 2 are correct, but the former cannot be used to justify the latter (at least at LHC energies). It is also clear that statement 2 alone cannot be used to justify statement 1. The factorization formula is given by the convolution of parton densities with partonic cross sections, and information on the former is not enough to justify statement 1. But it is usual to encounter the claim that, due to the high number of gluons, heavy quark production is dominated by the gluon fusion process. Implicitly, it assumes that the ratio of partonic cross sections $\hat{\sigma}^{ij\to Q+X}$ is close to one. However, at LHC and RHIC energies, the ratio $\hat{\sigma}^{Qg\to Qg}/\hat{\sigma}^{gg\to Q\bar{Q}}$ is large (around 60 at $p_t = 10$ GeV, $\sqrt{s} = 7$ TeV, and central rapidity). In 2002, Field showed that the main contribution is the Qg process [1]. A full calculation, based on the implementation of formula (1), using LO partonic cross sections and CTEQ PDFs [12], is shown in Fig. 3. We can see that, for the charm quark, the Qg contribution is approximately 4 times larger than the gg contribution, and 3 times larger for the bottom. It was in fact expected, looking at the ratios

[4]Strictly speaking, we should say below the NLO calculations, but we have seen that $p_t \backsimeq 5 - 10m_Q$. See also the NLO results compared to FONLL, Fig. 4.

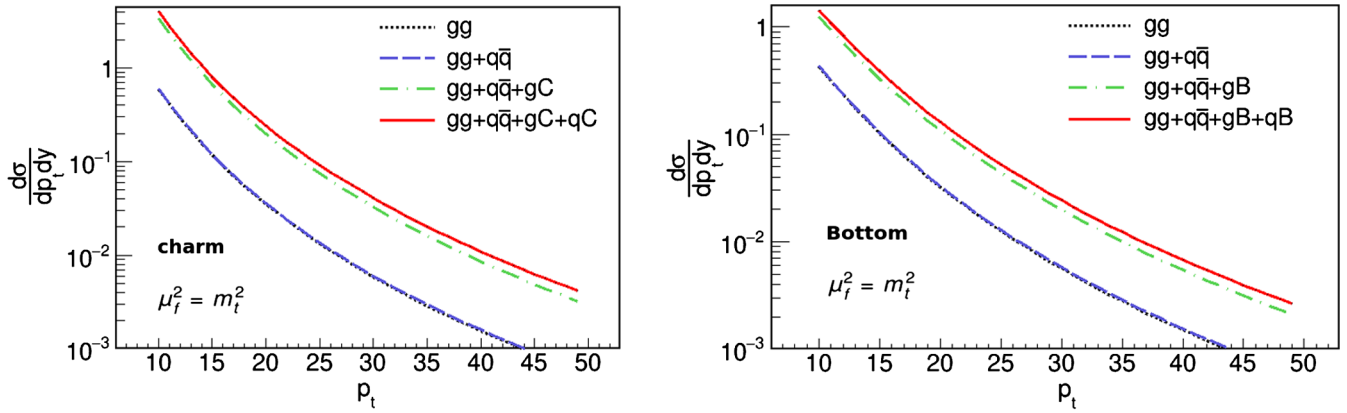

FIG. 3. Respective contributions for charm and bottom production. These cross sections are given for $-0.5 < y < 0.5$ and the unit is the μb. The dotted black and dashed blue lines are superposed due to the small $q\bar{q}$ contribution.

$g(x, Q^2)/Q(x, Q^2)$ and $\hat{\sigma}^{Qg\to Qg}/\hat{\sigma}^{gg\to Q\bar{Q}}$, and taking into account the factor 2 for the Qg contribution (the gluon can be provided by hadron 1 or hadron 2).

Finally, let us analyze statement 4. We have already seen that it is true in the FFNS. However, it is not the case in the VFNS, thanks to the heavy-quark density, resuming to all orders large logarithms, and to the flavor excitation diagrams, having large cross sections. In Fig. 4, we present the results obtained with the collinear factorization at LO, for the full contribution (solid red line) and for the gg contribution only (dotted black line). Using a factor $K = 1$, the full contribution is in very good agreement with NLO[5] and FONLL (for the bottom distribution) calculations obtained from [15]. In the case of charm production, the reason why NLO and our calculations are above the FONLL line is probably because of the absence of resummation of final state emissions. In the region $p_t > m_Q$, the gluon fusion contribution completely undershoots the FONLL result. Thinking that the main contribution is given by the gg process, and looking at the LO result (dotted black line), it is natural to think that at LO, one needs a large K factor. After adding the Qg and Qq contributions, everything is in order. We will see that the situation is similar within k_t factorization.

III. STANDARD HEAVY-QUARK PRODUCTION WITHIN k_t FACTORIZATION

In order to make the comparison with the collinear factorization easier, we rewrite Eq. (1) as

$$\frac{d\sigma}{dx_1 dx_2 d^2p_t}(x_1, x_2, p_t^2, Q^2, \mu^2) = \sum_{ij} f^i(x_1, Q^2; \mu^2) f^j(x_2, Q^2; \mu^2) \hat{\sigma}^{ij}(x_1, x_2, p_t^2). \quad (4)$$

Here, we do not consider the dependence on μ_R as for simplicity, α_s is taken constant. The factorization scale is now written μ and, using the freedom on the definition of parton densities, the logarithms of Q^2/μ^2 have been included in these functions. We keep track of μ in f^i and σ in order to keep in mind that, at finite orders, these quantities do depend on the factorization scale, giving rise to the factorization scale uncertainty.

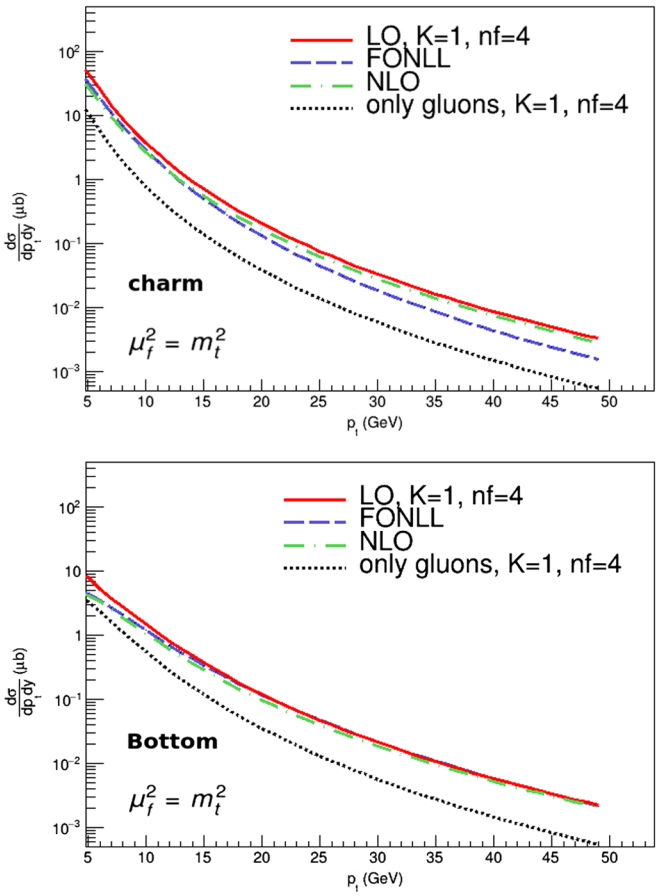

FIG. 4. Charm and bottom production, obtained with the formula (1), using LO partonic cross sections, LO CTEQ PDFs [12] and $K = 1$. This is in good agreement with NLO and FONLL results, obtained from the web page [15].

[5]The NLO result obtained from [15] is based on the Nason-Dawson-Ellis calculations [6].

The k_t factorization (also called high energy factorization or semihard approach) has been developed in parallel in Refs. [16–19], in order to resum the large logarithms of $\ln(1/x)$ which appear at high energies. For hadron-hadron collisions we have

$$\frac{d\sigma}{dx_1 dx_1 d^2p_t}(s, x_1, x_2, p_t^2, \mu^2) = \int^{k^2_{t,\max}} d^2k_{1t} d^2k_{2t} F(x_1, k_{1t}^2; \mu^2) F(x_2, k_{2t}^2; \mu^2) \times \hat{\sigma}(x_1 x_2 s, k_{1t}^2, k_{2t}^2, p_t^2), \quad (5)$$

with the variables x_1, x_2, p_t and μ having the same meaning as in Eq. (4). The first difference with the collinear factorization is the use of unintegrated parton densities (uPDF), depending on k_t, the transverse momentum of the spacelike incoming parton. This additional degree of freedom is integrated out, up to the kinematical upper bound $k^2_{t,\max}$, discussed in the Appendix. It is also sometimes necessary to have a specific treatment in the infrared region, see for instance Refs. [20,21]. In [16,17], the unintegrated gluon density obeys the Balitsky-Fadin-Kuraev-Lipatov (BFKL) equation [22], while in [19] the evolution is given by the nonlinear Balitsky-Kovchegov (BK) equation [23,24]. In the literature, some studies use Eq. (5) and the terminology k_t factorization, but employ uPDFs which do not obey the BFKL or BK equations. In order to keep the discussion as general as possible, we define the k_t factorization as the convolution of uPDFs with off-shell cross sections, without any condition on the x evolution. However, we will restrict to the cases where the uPDFs obey

$$f(x, Q^2; \mu^2) = \int^{Q^2} F(x, k_t^2; \mu^2) d^2k_t, \quad (6)$$

[or similar, see for instance Eq. (8)]. Here, we followed the notation used in Refs. [25,26].[6] We will also consider the uPDFs which are said to obey approximately Eq. (6).

The second difference with the collinear factorization is the use of off-shell partonic cross sections, which depend on the transverse momenta, k_{1t} and k_{2t}, of the incoming spacelike partons (with off-shellness $|k_i^2| \simeq k_{it}^2$). Outgoing partons are on shell.

Finally, a third difference, the main purpose of this paper, is the absence of the sum on parton types. The function $F(x, k_t^2; \mu^2)$ corresponds specifically to the unintegrated gluon density. This is for instance the case in the following papers [20,21,27–29]. Note that, in few cases, the role of the unintegrated quark density in different processes has been underlined and studied [30–32]. The off-shell cross section for the process $g^*g^* \to Q\bar{Q}$, where the stars indicate which parton is of shell, can be found in [17].

In Secs. V and VI, we will analyze heavy-quark production within k_t factorization. Before the discussion is in order, in Sec. IV we present some issues and complications with the use of k_t factorization.

IV. ON THE PRACTICAL USE OF THE k_t FACTORIZATION

The most problematic part comes from the uPDFs. We first note the existence of various conventions, making the comparison of different papers more complicated. In some cases, it is even not possible to know which convention has been used, in particular because the relation to the usual PDFs is not given. For instance, if the relation is

$$f(x, Q^2; \mu^2) = \int^{Q^2} F(x, k_t^2; \mu^2) dk_t^2, \quad (7)$$

then this uPDF is related to the one in Eq. (6) by a factor of π. Another convention is given below in Eq. (8). More important, in view of the next section, is the discussion of the uncertainties on these uPDFs. If one finds easily some theoretical explanations or references on how these uPDFs are built, details concerning the practical implementation are not always given. It is clear that the implementation of the same uPDF done by different groups can leave to differences in final results. In particular, the uPDFs built from the usual PDFs, like the KMR [33,34] uPDFs, depend on the choice of the PDF set. We believe that all groups should try to use the same sets of uPDFs,[7] making the comparison between different studies easier. For this reason, we think that the TMDlib [35] is a very good initiative. This is a library of uPDFs, and all the results of this paper will be obtained with uPDFs taken from it, when possible.

Another issue is the ambiguity of LO calculations, using only unintegrated gluon densities (uGDs). In this case, if not explicitly stated, it is not always possible to know if the calculation is performed using a FFNS, or using a VFNS with the approximation that the gg process gives the main contribution. We analyze separately these two cases in Secs. V and VI.

Since the parton densities are order and scheme dependent, different choices of schemes can result in quite different uPDFs. In Fig. 5, we show different uGDs, taken from the TMDlib [35], and integrated based on the relation

$$xg(x, \mu^2; \mu^2) = \int_0^{\mu^2} F(x, k_t^2; \mu^2) dk_t^2. \quad (8)$$

As a reference, we show the LO and NLO CTEQ14 PDF [12] as black lines. Not surprisingly, the PB-NLO-HERAI +II-2018-set1 (later referred to as PB uPDFs) is in perfect

[6] However, our function $F(x, k_t^2; \mu^2)$ is related to their function by a factor x.

[7] This is the case with the collinear factorization where some "official" sets are provided by collaborations like CTEQ.

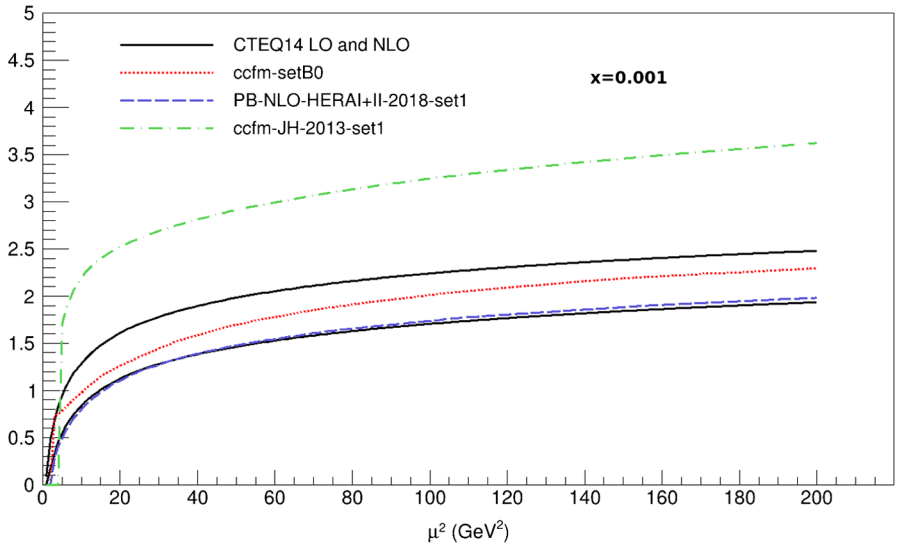

FIG. 5. CTEQ14 gluon distribution at LO (upper black line) and NLO (lower black line) [12], compared with integrated uPDFs taken from the TMDlib [35]: ccfm-JH-2013-set1 [36], ccfm-setB0 [37] and PB-NLO-HERA+II-2018-set1 [38]. These uPDFs are integrated out following Eq. (8).

agreement with the NLO CTEQ gluon, since it has been obtained in a VFNS with the Dokshitzer-Gribov-Lipatov-Altarelli-Parisi (DGLAP) evolution at NLO. In the opposite, the ccfm-JH-2013-set1 (later referred to as JH uPDFs) is a factor ∼2 above the CTEQ gluons. It is not an issue, and it was in fact expected, since the JH uPDFs have been determined using a nearly[8] 0-flavor scheme. Moreover, the CCFM uPDFs are sometimes said to obey only approximatively to the relation Eq. (8).

In the next sections, we discuss heavy-quark production within the k_t factorization. We will consider separately FFNS and VFNS calculations.

V. k_t FACTORIZATION WITH A FFNS

Because the CCFM evolution includes only gluons, calculations using CCFM uGDs is a typical example of FFNS. More precisely, in this case, a 0-flavor scheme. In Sec. II A, we have seen that LO FFNS gluon densities able to reproduce heavy-quark data at large energies, could be quite larger than NLO FFNS or LO VFNS gluons. It is then not surprising for the JH uPDFs to be above the CTEQ gluons. After including the NLO contributions in the off-shell cross section, we can expect the CCFM uGDs to be divided by a large factor, $K \simeq 2$, similarly to the collinear factorization case.[9] In the next section, it will be explained why the ccfm-setB0 uPDFs (later referred as to B0 uPDF) are smaller than the JH uPDFs.

For reasons identical to the collinear factorization case, these calculations suffer from large uncertainties, related to the uGDs and scales variation. The result could be improved, either by including NLO contributions or by changing to a VFNS.[10] An equivalent statement is that taking into account the unintegrated heavy-quark density will improve the result.

VI. k_t FACTORIZATION WITH A VFNS

In the previous section, we discussed that the 0-flavor scheme calculations, which include only the gg contribution, are correct but suffer from large uncertainties. Here, the situation is completely different. A VFNS calculation should take into account the flavor excitation processes. Including only $gg \to Q\bar{Q}$ means that the Qg and Qq contributions are considered to be negligible.

In Sec. VI A, we show that this is wrong, and that, similarly to the collinear factorization, the main contribution is given by $Qg \to Qg$. Then, in Secs. VI B and VI C, we show that, if available VFNS calculations are in agreement with data, it is because they (effectively) include a large K factor.

We claim and we will show that, if the gg contribution alone is in agreement with data, the full calculation, including in particular the Qg process will completely overshoot the data.

A. Main contribution and large K factor

In Sec. II C, we have seen that in the VFNS at LO, no large K factor is required. We argue that this is also true for

[8]The authors have modified the Ciafaloni-Catani-Fiorani-Marchesini (CCFM) evolution in order to include valence quarks [36].

[9]One of the reasons explaining the similarities between k_t and collinear factorization is that, in the limit $k_t \ll p_t$, the off-shell cross sections reduce to the usual ones.

[10]It is possible to modify the CCFM evolution in order to include valence and sea quarks [36].

k_t factorization. Two reasons why no large K factor is required are:

(1) The arguments given in Sec. II C are still valid: the flavor excitation cross sections are large and the unintegrated heavy-quark density resums large logarithms.
(2) Once we take into account all contributions, we obtain a result in good agreement with NLO calculations, see Fig. 12 and the associated discussion.

In Fig. 6 are shown the contributions $gg \to c\bar{c}$, $cg \to cg$ and $cq \to cq$ to the charm p_t distribution, obtained with KaTie [39] and the PB uPDFs. The unintegrated gluon distribution from this set has already been presented in Fig. 5. The reason why the labels are sg and qs rather than cg and qc is because heavy quarks in the initial state are not allowed in KaTie. Consequently, we have used $s(x,\mu^2)/1.3$ which is in fact a quite good charm quark, as shown in the bottom panel of Fig. 6. It has been checked that the factor 1.3 does not change to much with x. Last detail: for the calculation of the contributions shown in the top panel of Fig. 6, the factorization scale $\mu = (p_t^c + p_t^X)/2$ is used, where c refers to the charm and X to the other outgoing particle. Since we start the calculation for $p_t^c = 4$ (and for a technical reason $p_t^X > 2$), then $\mu^2 \geq 9\,\mathrm{GeV}^2$. Consequently, there is no issue with the behavior of the PDFs at small μ^2, and it is acceptable to neglect the effect of the charm mass in the matrix elements for $cg \to cg$ and $cq \to cq$.

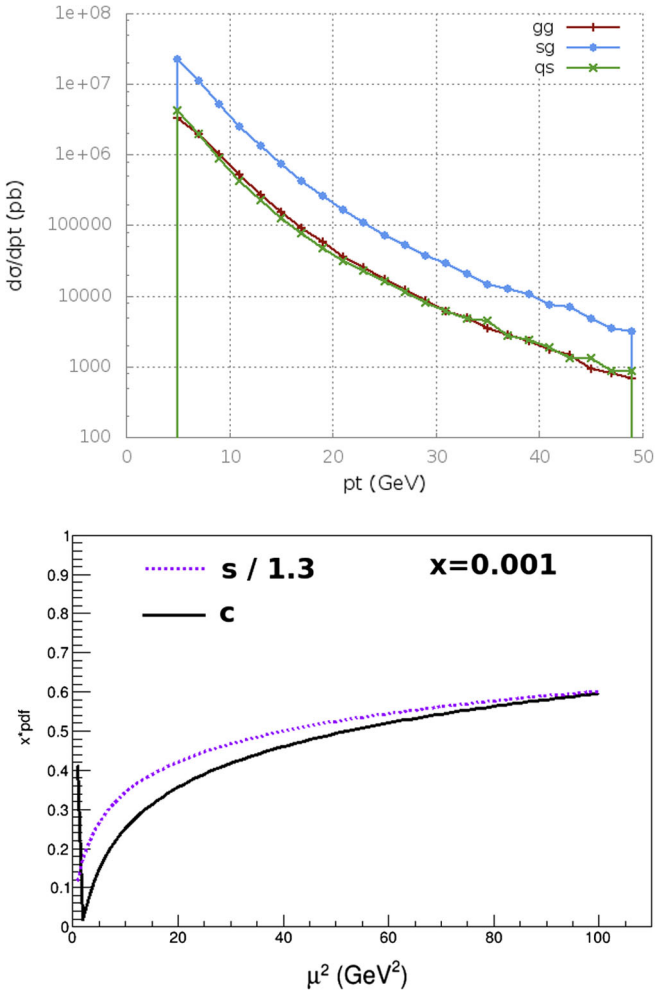

FIG. 6. Top panel: gg, cg and qc contributions to the charm p_t distribution. Instead of the charm uPDF, the strange uPDF divided by 1.3 is used, because KaTie does not accept initial heavy states. See the text for more details. Bottom panel: comparison of $c(x,\mu^2)$ and $s(x,\mu^2)/1.3$.

It is clear that the use of $s(x,\mu^2)/1.3$ instead of the true charm distribution includes an uncertainty in our calculations. However, as it can be seen in Fig. 6, this uncertainty is of the order of 10%, and is irrelevant, since we are discussing the correctness of a large K factor.

The result shown in Fig. 6 is exactly what was expected from the theory. The cg contribution is a factor ∼4 larger than the gg contribution. This result has been obtained using public codes written by other groups. This is the method used in the case of collinear factorization, where there are few official PDFs, given by collaborations like CTEQ. The fact that some groups use their unpublished implementation of uPDFs makes it hard or impossible to reproduce their results. In particular, it is not possible to check if the used uPDFs respect the relation they are supposed to respect, and we will see that it is not always the case.

B. Discussion on published results

Calculations using uPDFs determined by the inversion of Eq. (8) are an example of VFNS calculations, since the usual PDFs have been obtained in this scheme. This is for instance the case of the KMR uPDFs, which is treated in detail in the next subsection. Using uPDFs determined in a VFNS and obeying to Eq. (8), it should be impossible to be in agreement with data, taking into account only the gg contribution. If the published results do, it is because they (effectively) include a large K factor. It can be done at least in four ways:

(1) Too large unintegrated gluon distribution, $g(x) \to \sqrt{K} g(x)$.
(2) Put by hand, in order to take into account supposedly large higher order corrections.
(3) By choosing the factorization scale much higher than the usual choice.
(4) Unreasonably large k_t tail, see Sec. VI C.

By too large uGDs, we mean that, after integrating the uGD with the appropriate formula, the result is a factor $\sqrt{K}$ larger than the appropriate gluon density. By appropriate gluon density, we mean a gluon density determined in a scheme and to an order identical to the uGD. Due to the lack of information and to the issues discussed in Sec. IV, it is not always possible to check if the used uPDFs are too large. Ideally, something similar to our Fig. 5 should be shown, in order to demonstrate that the uPDFs are correctly normalized. It is done in several papers using ccfm uPDFs,

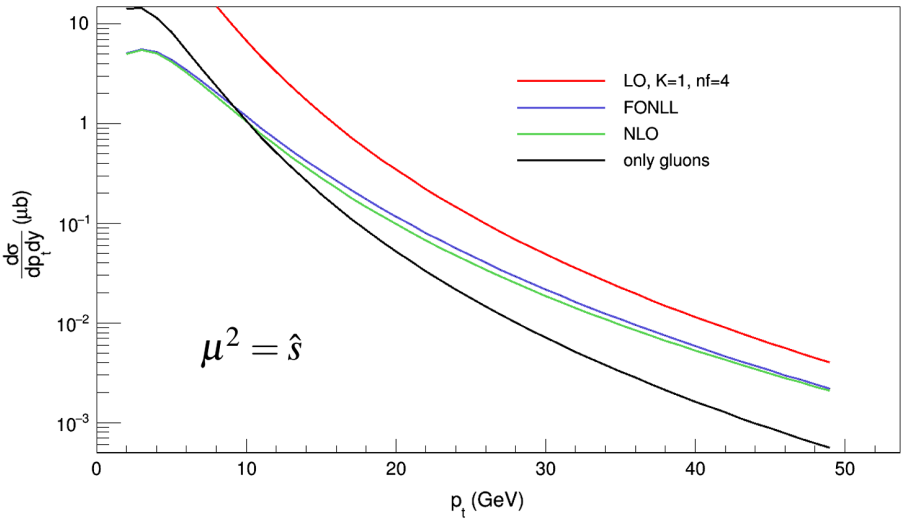

FIG. 7. Bottom production, obtained with the formula (1), using LO partonic cross sections, CTEQ PDFs, $K = 1$ and the factorization scale $\mu^2 = \hat{s}$.

see for instance [36]. However, in this case the issue is the lack of gluon densities determined at LO in a 0-flavor scheme,[11] necessary for a meaningful comparison.

The second possibility consists in adding a factor K by hand, in order to take into account higher order corrections. This factor is discussed for instance in Ref. [40] [Eq. (21)]. We have already seen that in the VFNS, no large K factor is required. To our knowledge, there is no evidence of the use of such a factor in recent studies based on the k_t factorization.

The third possibility consists in using uPDFs with a factorization scale much higher than the usual one, $\mu_F^2 \gg \mu^2 \sim p_t^2 + m^2$, with p_t^2 the transverse momentum of the outgoing parton and m the heavy-quark mass. It is for instance the case in Ref. [29], where the authors use $\mu_F^2 = \hat{s} + k_t^2$, ($\hat{s} = x_1 x_2 s$) and the B0 uPDFs,[12] plotted in Fig. 8. In the case of collinear factorization, it is clear that choosing a much higher factorization scale gives an effective large K factor. Indeed, while physical observables computed to all orders do not depend on the factorization scale, in finite order calculations, and in particular at LO, the dependence on μ can be significant. In Fig. 7, we show the same calculations as in Fig. 4, now using $\mu^2 = \hat{s}$. Even if this factorization scale is still smaller than the one in Ref. [29], we see that the gg contribution alone is in better agreement with FONLL, while the full contribution is too high.

[11]We have already mentioned that we expect this gluon density to be quite larger than the CTEQ gluons.

[12]It could look incoherent to mention ccfm uPDFs in this section dedicated to the VFNS. However, here it is just a numerical matter. The reason why the B0 uGD, 2 times smaller than the JH uGD, gives an acceptable result is because they are used with a very large factorization scale, effectively giving a large K factor.

Moreover, the factorization scale $\mu_F^2 = \hat{s} + k_t^2$ is not appropriate for two reasons. First, it should not be defined as a function of k_t^2. Indeed, for uPDFs obeying Eq. (8) (or equivalent), it gives the impossible equation:

$$xg(x, \hat{s} + k_t^2) = \int^{\hat{s}+k_t^2} dk_t^2 F(x, k_t^2; \hat{s} + k_t^2). \tag{9}$$

Second, one should avoid defining the factorization scale as a function of x_1 and x_2, which are integration variables for the cross section $d\sigma/dp_t^2$. In Ref. [41] it is shown that this kind of choice for μ is dangerous (see the discussion on pages 20–22).

Finally, we also want to mention that for D-meson and B-meson production, the branching fraction used for the hadronization is not always indicated.

C. The case of the KMR/MRW parametrization

We have implemented the KMR uPDFs (to be exact, the MRW uPDFs [34], also used in [27]), using the CTEQ14 LO PDFs. For the gluon, the expression is

$$\begin{aligned} F_g(x, k_t^2, \mu^2) &= T_g(k_t^2, \mu^2) \frac{\alpha_s(k_t^2)}{2\pi k_t^2} \times \int_x^1 dz \left[\sum_q P_{gq}(z) \frac{x}{z} q\left(\frac{x}{z}, k_t^2\right) \right. \\ &\left. + P_{gg}(z) \frac{x}{z} g\left(\frac{x}{z}, k_t^2\right) \Theta\left(\frac{\mu}{\mu + k_t} - z\right) \right], \end{aligned} \tag{10}$$

with P_{ij} the unregularized splitting functions, and T_g the Sudakov form factor:

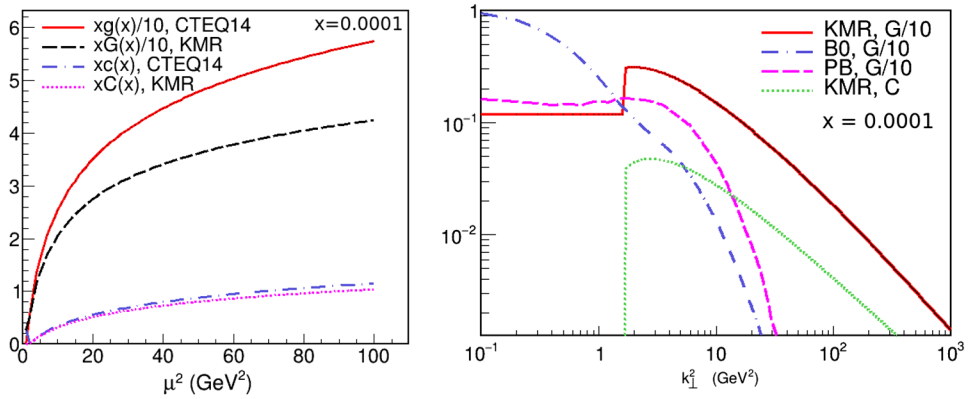

FIG. 8. Left: based on Eq. (8), the KMR uPDFs for charm and gluon are integrated and compared to LO CTEQ14 PDFs. Right: k_t^2 distribution of the KRM uPDFs at $\mu^2 = 10$ GeV^2 and $x = 10^{-4}$. For comparison, we also show the result of the ccfm-setB0 and PB-NLO-HERA+II-2018-set1 sets. All the gluon distributions have been normalized by 10.

$$T_g(k_t^2,\mu^2) = \exp\left(-\int_{k_t^2}^{\mu^2} dq^2 \frac{\alpha_s(q^2)}{2\pi q^2}\left(\int_0^{1-\Delta} dz z P_{gg}(z) + n_f\int_0^1 dz P_{qg}(z)\right)\right). \quad (11)$$

Note the factor z in front of the P_{gg} splitting function, absent in [33] [Eq. (3)]. This factor regularizes the divergence of the P_{gg} splitting function at $x = 0$. In order to avoid the divergence at $x = 1$, this parametrization uses $z_{\max} = 1 - \Delta$, with

$$\Delta = \frac{k_t}{k_t + \mu}. \quad (12)$$

In Fig. 8 we show the result of the implementation at $x = 10^{-4}$. In the left panel, we checked that this parametrization indeed respects the relation (8). For gluons, there is a discrepancy of ∼25%, due to the introduction of Δ, not dictated by the DGLAP equation [42]. In the right panel, we show the k_t^2 distribution. We have a very similar shape compared to [27], but our distribution is smaller. It could be due to the fact that we use the CTEQ PDFs, while the authors of [27] use the MSTW08 PDFs [43].

Using our MRW uPDFs and the KaTie event generator, it came as a big surprise to see that the gg contribution alone gives a good description of NLO calculations for the charm p_t distribution, as illustrated in Fig. 9. However, as explained before, it is not good news since, after adding the gQ contribution, the result will completely overshoot the NLO line.

In the following, we will demonstrate that this agreement is accidental. It is related to the definition of Δ, Eq. (12), and to the fact that this specific implementation of uGD obeys Eq. (8) only approximately, as shown in Fig. 8. At $k_t = \mu$, $z_{\max} = 0.5$, and because the parametrization allows $k_t > \mu$ (giving a Sudakov form factor larger than one), $z_{\max}$ can even go to zero, an unrealistic value [in Eq. (11), P_{qg} is integrated up to $z = 1$]. Using instead

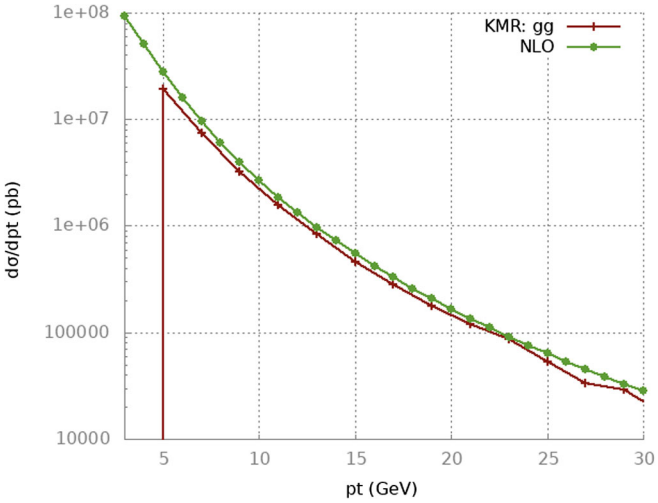

FIG. 9. NLO calculation for the charm p_t distribution, compared to $gg \to c\bar{c}$ using KMR gluons.

$z_{\max} = 0.99$, in Eqs. (10) and (11), we obtained a much better agreement between the CTEQ and the integrated KMR gluon densities, see Fig. 10 (left). However, in this case, the gg contribution overshoots the NLO line by more than 1 order of magnitude (see Fig. 10, right), showing that the previous agreement was just accidental.

The reason for the too large gg contribution, both in Figs. 10 and 9, is the large k_t tail of the KMR parametrization. Here, by large we precisely mean $k_t^2 > \mu^2$. This part of the distribution is not constrained by the relation (8). While the other uPDFs displayed in Fig. 8 show a very fast decrease at $k_t^2 \gtrsim \mu^2$, the KMR uPDFs decrease slower. To probe the contribution of this large k_t tail, we set the uPDFs equal to zero[13] for $k_t^2 > 1.5\mu^2$. The result obtained with these cut KMR uPDFs is shown in

[13]We did not choose to set these functions to zero for $k_t^2 > \mu^2$ because, compared to the other uPDFs displayed in Fig. 8, it would have been too rough.

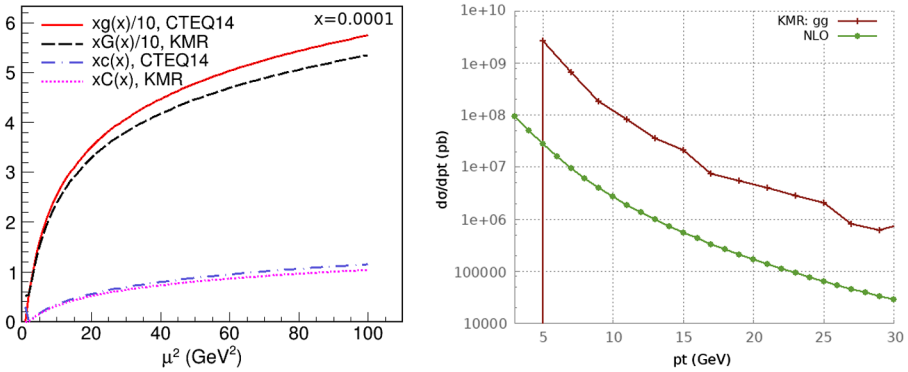

FIG. 10. Same as Figs. 8 (left) and 9, with $z_{\max} = 0.99$ ($\Delta = 0.01$).

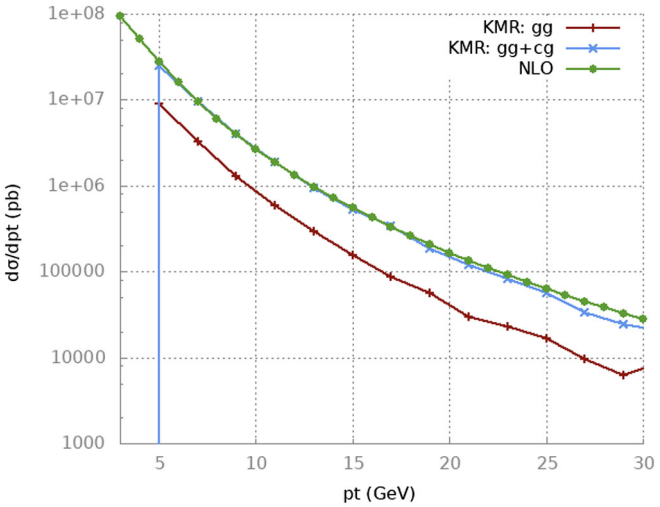

FIG. 11. NLO calculations for the charm p_t distribution, compared to the gg and $gg + cg$ contributions, using our cut KMR uPDFs.

Fig. 11. The gg contribution is now below the NLO line, showing that indeed, the large k_t tail gives an important contribution. Note also the good agreement of the $gg + cg$ calculation. Clearly, this agreement depends on our choice for the cut KMR uPDFs. What really matters is the confirmation that the Qg process gives the dominant contribution.

We believe that the KMR large k_t tail cannot be correct for the following reason. In the KMR paper [33], the uPDFs are built in two steps. In the first step, inverting Eq. (8) and using the DGLAP equation gives

$$k_t^2 F_a(x,k_t^2,\mu^2) = \left.\frac{\partial a(x,\mu^2)}{\partial \ln \mu^2}\right|_{\mu^2=k_t^2} = \frac{\alpha_s}{2\pi}\sum_{a'}\left[\int_x^{1-\Delta} P_{aa'}(z)a'\left(\frac{x}{z},k_t^2\right)dz - a(x,k_t^2)\int_0^{1-\Delta} P_{a'a}(z)dz\right], \quad (13)$$

with $a(x,\mu^2)$ the usual momentum density. The term with a minus sign is referred to as the virtual contribution. In a second step, this virtual contribution disappears, replaced by the Sudakov form factor, supposed to resum the virtual contribution. It is clear that this Sudakov form factor does not play its role in the region $k_t^2 > \mu^2$, and while the virtual contribution can be large, leading to a substantial reduction of the first term in the rhs of Eq. (13), the Sudakov form factor (replacing the virtual contribution) multiplies this term by a factor larger than 1. This explains the slow decrease of the KMR uPDFs with k_t^2.

To summarize, with the KMR uPDFs, the agreement of the gg contribution with the NLO result is accidental. The unintegrated gluon does not exactly respect Eq. (8), and, trying to improve the situation by playing with $z_{\max}$ makes the gg contribution overshoot the NLO line. This overestimation is due to the too large k_t tail of the KMR uPDFs. Consequently, the result displayed in Fig. 9 cannot be considered as viable. Having a too large k_t tail could be seen as another way of implementing a large K factor.

D. Full calculation with KaTie and discussions

By employing a VFNS, we have seen that the main contribution to the heavy-quark p_t distribution is the process $Qg \to Qg$, both within collinear and k_t factorization. Equation (5) should be changed for

$$\frac{d\sigma}{dx_1 dx_1 d^2p_t}(s,x_1,x_2,p_t^2,\mu^2) = \sum_{ij}\int^{k^2_{\max}} d^2k_{1t}d^2k_{2t}F_i(x_1,k_{1t}^2;\mu^2)F_j(x_2,k_{2t}^2;\mu^2) \times \hat{\sigma}^{ij}(x_1x_2s,k_{1t}^2,k_{2t}^2,p_t^2), \quad (14)$$

where a sum on all parton types has been included. If all contributions are taken into account, no large factor is required. The result for the full calculation, using the PB

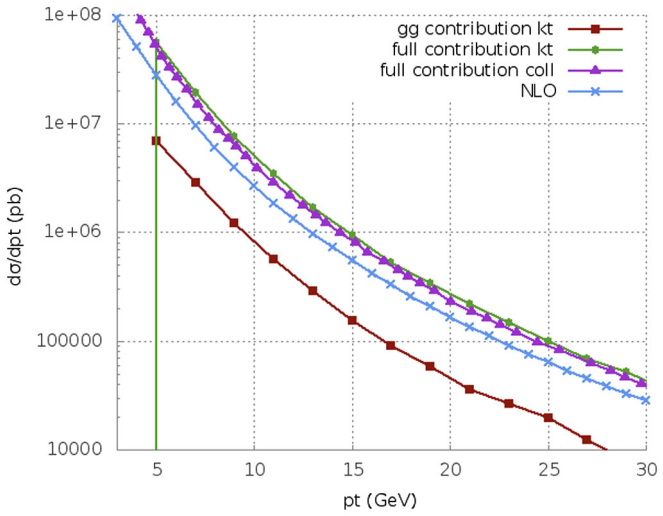

FIG. 12. Transverse momentum distribution of a charm quark at central rapidity. Results obtained with the KaTie event generator for the gg and the full contributions are compared with NLO calculations [15] and our collinear calculations.

uPDFs and the event generator KaTie is displayed in Fig. 12. The details of the implementation have already been presented in Sec. VI A. While the full calculation is in good agreement with NLO, the gg contribution alone is below the NLO line by a factor ∼4. These calculations also confirm that at medium and large p_t, collinear and k_t factorizations are numerically close (see [3,44]).

These numerical results confirm the theoretical expectations, and in particular, the importance of the gQ contribution. This conclusion can be probably generalized to several phenomenological papers using the k_t factorization. The majority of these papers take into account only the unintegrated gluon density $F_g(x, k_t; \mu)$, while it is likely that the unintegrated quark density, $F_q(x, k_t; \mu)$, also plays a non-negligible role in some of these studies. It is then important to systematically explore the effect of the quark contribution.

Concerning the phenomenology, the $Qg \to Qg$ process gives kinematical configurations quite different from the $gg \to Q\bar{Q}$ process. Including the flavor excitation contributions, as well as spacelike and timelike cascades, is the minimal requirement for a realistic comparison with observables like heavy-quarks correlations.[14] Note that, in the framework of models based on collinear factorization, the azimuthal correlations between a $b\bar{b}$ pair have been studied in [1], using the event generators HERWIG, ISAJET and PYTHIA. They observed that the toward region ($\Delta\phi \in [0, 90]$) is very sensitive to the presence of the flavor excitation and cascades processes.

[14]If the observable has been chosen in order to make the contribution of multiple partonic interactions (MPI) negligible. Otherwise a model for MPI should be implemented for realistic studies.

VII. CONCLUSION

We have analyzed the p_t distribution of a heavy quark in the fixed-flavor-number scheme and in the variable-flavor-number scheme. In Sec. II, discussing the case of collinear factorization, we reminded that in the FFNS, the NLO contributions give a large K factor, due to the opening of the flavor excitation channel. In the opposite, this is not true in the VFNS, since flavor excitation and the heavy-quark density, resuming to all orders large logarithms of $\ln(p_t^2/m_Q^2)$, are included at leading order.

The main goal of this paper was the discussion of the fact that, generally, k_t-factorization calculations include only the $gg \to Q\bar{Q}$ contribution. The conclusion of the discussion depends on the scheme used. We have seen that in a FFNS, taking into account only the gg contribution is correct, by definition for a 0-flavor scheme. For n-flavor schemes, with $n > 0$, it is a good approximation since the $q\bar{q} \to Q\bar{Q}$ contribution is negligible at small and medium x. However, in this scheme, the calculations suffer from large uncertainties. Moreover, in the region $p_t \gg m_Q$, NLO FFNS calculations fail and the heavy-quark density has to be taken into account for accurate predictions. In a VFNS, the unintegrated sea-quark densities should be taken into account, and we have shown that the $Qg \to Qg$ process gives the main contribution, for $p_t > m_Q$. Calculations in agreement with data and taking into account only the gg contribution are incorrect since (1) by definition of the VFNS, flavor excitation processes should be included and (2) if they were, the obtained result would overshoot data by a large factor (in the region $p_t > m_Q$).

In this scheme, if the gg contribution is in agreement with data, it is because the calculation (effectively) includes a large K factor. In Secs. VI B and VI C, we discussed how this factor can be implemented. It can be added by hand, or can be obtained by using a too large unintegrated gluon density, a too large factorization scale or uGDs with a too large k_t tail. We have shown that the latter possibility is the case of the KMR uPDFs.

In Sec. VI D, numerical (VFNS) calculations, done with the help of the KaTie event generator and the PB uPDFs have been presented in Fig. 12. They show that, while the gg contribution is far below the NLO line, the full contribution is in fair agreement with NLO calculations. We chose these uPDFs because they are part of the tmdlib library and because we have been able to check that they do obey the relation they are said to obey, e.g., Eq. (8). It is not the case of the KMR parametrization studied in Sec. VI C, where the uGD shows a disagreement of ∼25% with the corresponding gluon density. It is also interesting to note that, for the p_t distribution of a heavy quark, collinear

and k_t-factorization results are numerically very close, in agreement with [3,44].

Heavy-quark production is probably not an isolated case, and the role of unintegrated quark densities should be systematically studied in papers using the k_t factorization.

ACKNOWLEDGMENTS

We would like to thank Andreas van Hameren for his help with the event generator KaTie. We are also grateful to Klaus Werner, Martin Hentschinski, Francesco Hautmann and Hannes Jung for their comments on the manuscript. We acknowledge support from Chilean FONDECYT iniciacion Grant No. 11181126. We acknowledge support by the Basal Project No. FB0821.

APPENDIX: KINEMATICAL UPPER BOUND

The upper bound for the k_t^2 integration is generally not important, since large k_t are suppressed by the unintegrated parton densities, $F(x, k_t^2)$. Sometimes, one finds the condition

$$(k_1 + k_2)^2 < s, \tag{A1}$$

with $k_1 = [k_0, \vec{k}_t, k_z]$ and $k_2 = [k_0, -\vec{k}_t, -k_z]$, in the partonic center-of-momentum frame. These partons being spacelike, we define

$$k_1^2 = k_2^2 = -Q^2. \tag{A2}$$

The condition (A1) is clearly insufficient since here, k_t can go to infinity without violation of this bound or of energy conservation. Indeed, using the approximation $k_t^2 = Q^2$ (used in the calculation of off-shell cross sections) we get

$$k_0^2 = -Q^2 + k_t^2 + k_z^2 = k_z^2, \tag{A3}$$

and the energy is finite. Intuitively, the upper bound would be

$$k_{t,\max}^2 = \frac{s}{4}. \tag{A4}$$

In the case of on-shell particles, in order to find the upper bound for p_t, one writes an equation for 4-momentum conservation and put p_z to zero. This is how the upper bound $p_t^2 < \hat{s}/4$ is found. Trying to do the same in the case of off-shell particles, we first get

$$(k_1 + k_2)^2 = \hat{s} = 4k_0^2, \tag{A5}$$

giving the usual relation $k_0^2 = \hat{s}/4$. The second step consists in writing explicitly the relation (A2):

$$k_t^2 + k_z^2 = \frac{\hat{s}}{4} + Q^2. \tag{A6}$$

In the case of on-shell partons, $Q^2 = 0$, taking k_z to zero gives $k_{t,\max}^2 = \hat{s}/4$. However, in the case of off-shell partons with $k_t^2 = Q^2$, the relation becomes

$$k_z^2 = \frac{\hat{s}}{4}. \tag{A7}$$

We see that it is not possible to obtain the upper bound in this way.

We need to find another method for the derivation of the upper bound $k_{t,\max}^2$. First, we want to show that the relation $k_t^2 = Q^2$ cannot be correct. We will see that this is an approximation, accurate only in a specific kinematical region. Let us consider the diagram in Fig. 13. Here, we consider the simplified situation where the spacelike parton is generated after the bremsstrahlung from a perfectly collinear on-shell parton with energy

$$E = \frac{\sqrt{s}}{2}. \tag{A8}$$

For the spacelike parton, we choose the parametrization $k = [xE, \vec{k}_t, xE]$, which corresponds to the approximation $k^2 = -Q^2 = -k_t^2$. But then, 4-momentum conservation implies that the radiated parton has the 4-momentum

$$p = [(1-x)E, -\vec{k}_t, (1-x)E]. \tag{A9}$$

This is not acceptable since it gives $p^2 = -k_t^2 < 0$ and we want the radiated parton to be timelike or on shell. This strange situation is due to the approximation $Q^2 = k_t^2$.

Relaxing this approximation and using the same diagram, it is in fact possible to derive the true relation between k_t^2 and Q^2, as well as the upper bounds for these two quantities. 4-momenta can be written

$$q = (E, 0, 0, E) \tag{A10}$$

$$k = (E_k, \vec{k}_t, k_z) \tag{A11}$$

$$p = (E_p, -\vec{k}_t, p_z). \tag{A12}$$

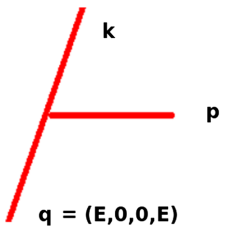

FIG. 13. p is the 4-momentum of the radiated parton while k is the 4-momentum of the spacelike parton. q is the proton (or parton with $x = 1$) 4-momentum.

Asking for 4-momentum conservation and choosing the radiated parton on shell gives the following equations:

$$E_p^2 = k_t^2 + p_z^2 \tag{A13}$$

$$E_k + E_p = E \tag{A14}$$

$$k_z + p_z = E. \tag{A15}$$

With these equations, we obtain

$$E_k + \sqrt{k_t^2 + (E - k_z)^2} = E \tag{A16}$$

$$E_k^2 - k_t^2 - k_z^2 = 2E(E_k - k_z). \tag{A17}$$

In the lhs of Eq. (A17), one can recognize $k^2 = -Q^2$. We then obtain the following expression for the virtuality:

$$Q^2 = 2E(xE - E_k), \tag{A18}$$

where the definition $k_z := xE$ has been used. The maximum value is obtained for $E_k = 0$:

$$Q^2_{\max}(x) = 2xE^2 = \frac{xs}{2}, \tag{A19}$$

giving the x-dependent upper bound for the virtuality.

The relation between k_t^2 and Q^2 can be obtained using Eq. (A16) and the off-shell condition $E_k^2 - k_t^2 - k_z^2 = -Q^2$, giving

$$k_t^2 = Q^2(1 - x) + \frac{Q^4}{s}, \tag{A20}$$

where we have used the fact that $4E^2 = s$ and $k_z = xE$. We see that in the limit $Q^2/s \ll (1 - x)$ and $x \ll 1$, this equation reduces to

$$k_t^2 = Q^2. \tag{A21}$$

Using Eq. (A19), we see that $Q^2/s \ll (1 - x)$ is always true at small x. Then, the condition $x \ll 1$ is enough to ensure the validity of the approximation Eq. (A21), showing that at small x, it is justified to use this relation when computing the off-shell cross section.

As for Q^2, the upper bound for k_t is obtained in the case $E_k = 0$. Inserting Eq. (A19) in Eq. (A20), we obtain

$$k^2_{t,\max}(x) = \frac{s}{4}(2x - x^2). \tag{A22}$$

At small x, corresponding to the kinematical region of interest for the k_t factorization, we have

$$k^2_{t,\max}(x) \simeq \frac{xs}{2}. \tag{A23}$$

For $x = 1$, one has $k^2_{t,\max} = s/4$, which is the x-independent intuitive expectation given in Eq. (A4). This limit corresponds to the simple case where the radiated parton takes all the energy and has no longitudinal momentum, $p = [E, \vec{E}, 0]$. Then the 4-momentum of the spacelike parton is $k = [0, \vec{E}, E]$, showing that the parametrization $[xE, \vec{k}_t, xE]$ can be really incorrect. In this case we have $k_t^2 = \frac{Q^4}{s} \neq Q^2$. Of course, the probability for an emission with a very large transverse momentum is low, and the region of large x is supposed[15] to be outside of the domain of applicability of the k_t factorization.

Finally, we wonder if the upper bound is always irrelevant, if we are only interested by the main contribution. In Ref. [3], it is shown that doing the integration up to p_t^2 (or $m_t^2 = p_t^2 + m^2$), p_t being the transverse momentum of the outgoing parton, is enough in order to obtain the main contribution. If $k^2_{t,\max} > p_t^2$ or $1 \ll k^2_{t,\max} < p_t^2$, the upper bound is irrelevant.[16] Then, we concentrate on the small-p_t and small-x region and wonder when

$$k^2_{t,\max}(x_{1,2}) \simeq \frac{x_{1,2}s}{2} = p_t^2, \tag{A24}$$

with

$$x_1 = \frac{p_{1,t}}{\sqrt{s}}e^{y_1} + \frac{p_{2,t}}{\sqrt{s}}e^{y_2} \qquad x_2 = \frac{p_{1,t}}{\sqrt{s}}e^{-y_1} + \frac{p_{2,t}}{\sqrt{s}}e^{-y_2}, \tag{A25}$$

and we choose $p_{1,t} = p_t$, while $p_{2,t}$ is integrated out. Let us take the case of x_1. We have

$$\frac{x_1 s}{2} = \frac{\sqrt{s}}{2}(p_t e^{y_1} + p_{2,t}e^{y_2}) = p_t^2. \tag{A26}$$

The solution is

$$p_t = \frac{\sqrt{s}}{4}e^{y_1}\left(1 + \sqrt{1 + 8\frac{p_{2,t}}{\sqrt{s}}e^{y_2 - 2y_1}}\right). \tag{A27}$$

Let us consider that small p_t means $p_t = 1$ GeV, then the two factors in the rhs of Eq. (A27) have to be

[15]Computing $d\sigma/dp_t$ requires an integration over x which is not restricted to small values. We do not know if the region of, let us say $x > 0.01$, gives a negligible contribution.

[16]The second case is due to the fact that large k_t contributions are strongly suppressed by $F(x, k_t^2)$, the unintegrated parton densities.

small. If the term with $p_{2,t}$ is negligible, the condition on y_1 is

$$\frac{\sqrt{s}}{2} e^{y_1} = 1, \tag{A28}$$

which corresponds to the value $y_1 \sim -8.16$, for $\sqrt{s} = 7\,\text{TeV}$. If the second term with $p_{2,t}$ is not negligible, the value will be even more negative. For Pb-Pb collision, $\sqrt{s}$ is smaller which gives a smaller value for y_1. Then, at the LHC, if one starts to measure particles at $y \sim 7$–8, $k^2_{t,\max}$ will play an important role, while at central rapidities, it does not.

It is maybe possible to find a more restrictive $k^2_{t,\max}$, for instance due to angular ordering. In this case, the absolute value of y, for which the precise definition of the upper bound plays a role, will be smaller.

[1] R. D. Field, Sources of b quarks at the Fermilab Tevatron and their correlations, Phys. Rev. D **65**, 094006 (2002).

[2] R. K. Ellis, W. J. Stirling, and B. R. Webber, *QCD and Collider Physics* (Cambridge University Press, Cambridge, England, 1996).

[3] B. Guiot, Hard scale uncertainty in collinear factorization: Perspective from k_t-factorization, Phys. Rev. D **98**, 014036 (2018).

[4] M. Cacciari, M. Greco, and P. Nason, The p(T) spectrum in heavy-flavour hadroproduction, J. High Energy Phys. 05 (1998) 007; The p(T) spectrum in heavy-flavor photoproduction, J. High Energy Phys. 03 (2001) 006.

[5] P. Nason, S. Dawson, and R. K. Ellis, The total cross section for the production of heavy quarks in hadronic collisions, Nucl. Phys. **B303**, 607 (1988).

[6] P. Nason, S. Dawson, and R. K. Ellis, The one particle inclusive differential cross section for heavy quark production in hadronic collisions, Nucl. Phys. **B327**, 49 (1989); Erratum, Nucl. Phys. **B335**, 260(E) (1990).

[7] W. Beenakker, H. Kuijf, W. L. van Neerven, and J. Smith, QCD corrections to heavy-quark production in $p\bar{p}$ collisions, Phys. Rev. D **40**, 54 (1989).

[8] W. Beenakker, W. L. van Neerven, R. Meng, G. A. Schuler, and J. Smith, QCD corrections to heavy quark production in hadron-hadron collisions, Nucl. Phys. **B351**, 507 (1991).

[9] M. A. G. Aivazis, J. C. Collins, F. I. Olness, and W.-K. Tung, Leptoproduction of heavy quarks. 2. A unified QCD formulation of charged and neutral current processes from fixed target to collider energies, Phys. Rev. D **50**, 3102 (1994).

[10] B. A. Kniehl, G. Kramer, I. Schienbein, and H. Spiesberger, Inclusive charmed-meson production at the CERN LHC, Eur. Phys. J. C **72**, 2082 (2012).

[11] B. A. Kniehl, G. Kramer, I. Schienbein, and H. Spiesberger, Inclusive B-meson production at small p_T in the general-mass variable-flavor-number scheme, Eur. Phys. J. C **75**, 140 (2015).

[12] S. Dulat, T.-J. Hou, J. Gao, M. Guzzi, J. Huston, P. Nadolsky, J. Pumplin, C. Schmidt, D. Stump, and C.-P. Yuan, New parton distribution functions from a global analysis of quantum chromodynamics, Phys. Rev. D **93**, 033006 (2016).

[13] B. A. Kniehl, G. Kramer, I. Schienbein, and H. Spiesberger, Inclusive B-meson production at the LHC in the GM-VFN scheme, Phys. Rev. D **84**, 094026 (2011).

[14] Y. V. Kovchegov and E. Levin, *Quantum chromodynamics at high energy* (Cambridge University Press, Cambridge, England, 2012).

[15] http://www.lpthe.jussieu.fr/ cacciari/fonll/fonllform.html.

[16] J. C. Collins and R. K. Ellis, Heavy-quark production in very high energy hadron collisions, Nucl. Phys. **B360**, 3 (1991).

[17] S. Catani, M. Ciafaloni, and F. Hautmann, High energy factorization and small-x heavy flavour production, Nucl. Phys. **B366**, 135 (1991).

[18] L. Gribov, E. Levin, and M. Ryskin, Semihard processes in QCD, Phys. Rep. **100**, 1 (1983).

[19] E. M. Levin, M. G. Ryskin, Y. M. Shabelski, and A. G. Shuvaev, Heavy quark production in semihard nucleon interaction, Sov. J. Nucl. Phys. **53**, 657 (1991).

[20] A. V. Lipatov, V. A. Saleev, and N. P. Zotov, Heavy Quark Production at the TEVATRON in the Semihard QCD Approach and the Unintegrated Gluon Distribution, arXiv:hep-ph/0112114v3.

[21] Yu. M. Shabelski, A. G. Shuvaev, and I. V. Surnin, Heavy quark production in k_t factorization approach at LHC energies, Int. J. Mod. Phys. A **33**, 1850003 (2018).

[22] E. Kuraev, L. Lipatov, and V. Fadin, Multiregge processes in the Yang-Mills theory, Sov. Phys. JETP **44**, 443 (1976); The Pomeranchuk singularity in nonabelian gauge theories, Sov. Phys. JETP**45**, 199 (1977); I. Balitsky and L. Lipatov, The pomeranchuk singularity in quantum chromodynamics, Sov. J. Nucl. Phys. **28**, 822 (1978).

[23] I. Balitsky, Operator expansion for high-energy scattering, Nucl. Phys. **B463**, 99 (1996).

[24] Y. V. Kovchegov, Small-x F_2 structure function of a nucleus including multiple Pomeron exchanges, Phys. Rev. D **60**, 034008 (1999).

[25] S. Catani, M. Ciafaloni, and F. Hautmann, Leptoproduction of heavy flavour at high energies, Nucl. Phys. B, Proc. Suppl. **29A**, 182 (1992).

[26] S. Catani, M. Ciafaloni, and F. Hautmann, Production of heavy flavours at high energies in *Hamburg 1991, Proceedings, Physics at HERA*, Vol. 2, pp. 690–711; *CERN Geneva–TH. 6398 (92/01)*, p. 21.

[27] R. Maciuła and A. Szczurek, Open charm production at the LHC-k_t-factorization approach, Phys. Rev. D **87**, 094022 (2013).

[28] H. Jung, Heavy quark production at the TEVATRON and HERA using k_t factorization with CCFM evolution, Phys. Rev. D **65**, 034015 (2002).

[29] H. Jung, M. Kraemer, A. V. Lipatov, and N. P. Zotov, Investigation of beauty production and parton shower effects at LHC, Phys. Rev. D **85**, 034035 (2012).

[30] S. Catani and F. Hautmann, Quark anomalous dimensions at small x, Phys. Lett. B **315**, 157 (1993).

[31] S. Catani and F. Hautmann, High-energy factorization and small-x deep inelastic scattering beyond leading order, Nucl. Phys. **B427**, 475 (1994).

[32] F. Hautmann, M. Hentschinski, and H. Jung, Forward Z-boson production and the unintegrated sea quark density, Nucl. Phys. **B865**, 54 (2012); TMD PDFs: a Monte Carlo implementation for the sea quark distribution, arXiv: 1205.6358; Unintegrated sea quark at small x and vector boson production, arXiv:1209.6305.

[33] M. A. Kimber, A. D. Martin, and M. G. Ryskin, Unintegrated parton distributions, Phys. Rev. D **63**, 114027 (2001).

[34] G. Watt, A. D. Martin, and M. G. Ryskin, Unintegrated parton distributions and inclusive jet productionat HERA, Eur. Phys. J. C **31**, 73 (2003).

[35] F. Hautmann, H. Jung, M. Krämer, P. J. Mulders, E. R. Nocera, T. C. Rogers, and A. Signori, TMDlib and TMDplotter: library and plotting tools for transverse-momentum-dependent parton distributions, Eur. Phys. J. C **74**, 3220 (2014).

[36] F. Hautmann and H. Jung, Transverse momentum dependent gluon density from DIS precision data, Nucl. Phys. **B883**, 1 (2014).

[37] H. Jung, Unintegrated parton density functions in CCFM, arXiv:hep-ph/0411287.

[38] A. B. Martinez, P. Connor, F. Hautmann, H. Jung, A. Lelek, V. Radescu, and R. Zlebcik, Collinear and TMD parton densities from fits to precision DIS measurements in the parton branching method, arXiv:1804.11152.

[39] A. Van Hameren, KaTie: For parton-level event generation with k_T-dependent initial states, Comput. Phys. Commun. **224**, 371 (2018).

[40] M. G. Ryskin, A. G. Shuvaev, and Yu. M. Shabelski, Comparison of k(T) factorization approach and QCD parton model for charm and beauty hadroproduction, Phys. At. Nucl. **64**, 1995 (2001).

[41] J. Collins, D. Soper, and G. Sterman, Factorization of hard processes in QCD, Adv. Ser. Direct High Energy Phys. **5**, 1 (1989).

[42] V. N. Gribov and L. N. Lipatov, Deep inelastic e p scattering in perturbation theory, Sov. J. Nucl. Phys. **15**, 438 (1972); G. Altarelli and G. Parisi, Asymptotic freedom in parton language, Nucl. Phys. **B126**, 298 (1977); Y. L. Dokshitzer, Calculation of the structure functions for deep inelastic scattering and e^+e^- annihilation by perturbationtheory in quantum chromodynamics, Sov. Phys. JETP **46**, 641 (1977).

[43] A. D. Martin, W. J. Stirling, R. S. Thorne, and G. Watt, Parton distributions for the LHC, Eur. Phys. J. C **63**, 189 (2009); Uncertainties on α_S in global PDF analyses and implications for predicted hadronic cross sections, Eur. Phys. J. C**64**, 653 (2009).

[44] E. M. Levin, M. G. Ryskin, Y. M. Shabelski, and A. G. Shuvaev, Heavy quark production in parton model and in QCD, Sov. J. Nucl. Phys. **54**, 1420 (1991).